Femtosecond pulse source based on soliton filtering from a supercontinuum generated in a microstructured fiber

J. Licea Rodríguez, K. Garay Palmett*, and R. Rangel Rojo
Centro de Investigación Científica y de Educación Superior de Ensenada,
Apartado Postal 2732, Ensenada B.C., 22860, México,
**Instituto de Ciencias Nucleares, Universidad Nacional Autónoma de México,*
Apartado Postal 70-543, México DF. 04510, México,
e-mail: jlicea@cicese.mx, karinerger@gmail.com, rrangel@cicese.mx

Recibido el 18 de marzo de 2010; aceptado el 25 de mayo de 2010

In this article we report the implementation of a tunable source of ultrashort pulses, based on the generation of a supercontinuum in a photonic crystal fiber, using sub-100 fs pulses from a Ti:sapphire oscillator, and filtering the soliton with the longest wavelength out of the continuum. Using a zero dispersion filtering system we were able to get a pulse duration close to the minimum possible for the soliton. The pulses obtained were continuously tunable in the 850-1100 nm range, and tuning was achieved by input pulse energy variation. We present a complete characterization of the filtered pulses and show that the experimental results have a qualitative agreement with theory.

Keywords: Optical solitons; ultrashort pulses; solitons in optical fibers.

En este artículo reportamos la implementación de una fuente sintonizable de pulsos ultracortos, basada en la generación de un supercontinuo en una fibra de cristal fotónico, usando pulsos de 100 fs de un oscilador de Ti:zafiro, y filtrando el solitón con la mayor longitud de onda del continuo. Usando un sistema de filtrado de cero dispersión pudimos obtener una duración del pulso cercana a la mínima posible para el solitón. Los pulsos obtenidos fueron continuamente sintonizables en el rango de 850-1100 nm, la sintonización se logró variando la energía de los pulsos de entrada. Presentamos una caracterización completa de los pulsos filtrados y mostramos que los resultados experimentales tienen buena coincidencia con la teoría.

Descriptores: Solitones ópticos; pulsos ultracortos; solitones en fibras ópticas.

PACS: 42.65.Tg; 42.65.Re; 42.81.Dp

1. Introduction

Supercontinuum generation (SCG) refers to the creation of a broadband light source due to the propagation of intense laser pulses in a nonlinear optical medium. SCG has found numerous applications in such diverse fields as spectroscopy [1], optical coherence tomography [2] and remote sensing [3], to mention a few. SCG in photonic crystal fiber (PCF) by ultrashort-pulse propagation has become a subject of intense study. This is mainly because the pulse energies required to generate a supercontinuum are low due to the ability of the PCFs to minimize dispersion at the pump wavelength, the long effective interaction length, and their high nonlinear coefficient γ [4–7].

It has been demostrated that in the anomalous dispersion regime ($\lambda_p > \lambda_{zd}$, with λ_p and λ_{zd} being the pump central wavelength and zero dispersion wavelength, respectively) if the incident pulse power is sufficiently high so that the pulse can evolve to a higher order soliton, the stable propagation condition is perturbed by the higher order dispersion and nonlinear effects. In such situation, the original pulse can break up in his fundamental constituents, which in turn are shifted towards lower frequencies due to Intrapulse Raman Scattering, a phenomenon known as soliton self-frequency shift (SSFS) [8, 9]. The shifting can be controlled by varying the pump power, fiber length and linear chirp of the initial pulse [8, 10, 11]. This mechanism has permitted the development of tunable ultrashort pulses sources in different spectral ranges into the near infrared [12, 13]. In particular, as fundamental solitons have a well-defined spectral shape, the power dependent shift can be used to produce a near-infrared tunable laser source after some spectral filtering and probably recompression.

Near-infrared pulsed sources are essential to implement nonlinear optical microscopy techniques such as two-photon scanning microscopy [14, 15], second-harmonic generation microscopy [16,17], and third-harmonic generation microscopy [18]. Nonlinear optical microscopy techniques have a wide variety of applications in biological sciences, including live cell and tissue imaging. These imaging techniques have different advantages, like being naturally confocal, avoiding UV bleaching of the specimen, enabling the observation of interfaces in some cases, and not needing toxic marker molecules in others. Light from a supercontinuum source has been used in several nonlinear microscopy schemes using the whole spectrum or even selecting a part of it [19–21]. Likewise, tunable non-solitonic radiation from a supercontinuum generated in a PCF has served as a source to excite fluorescence by two-photon absorption in a microscopy system [22]. However, the solitonic components of a supercontinuum have received less attention as possible sources for nonlinear optical microscopy.

In this article we report experimental results related with the generation of a supercontinuum in a PCF, from which the soliton with the longest wavelength is filtered out of the SC and used to construct a tunable ultrashort pulses source by varying the pump power. The pulse length of solitons at the fiber output was preserved by using a zero dispersion filtering system (ZDFS), which avoided temporal spreading of solitons during the filtering process. We present a complete characterization of the filtered pulses that are continuously tunable in the 850-1100 nm range. An important property of the proposed near-infrared pulsed source is that the soliton pulse energies obtained after filtering are large enough for applications in nonlinear microscopy. We also present theoretical results to compare with the experimental ones and determine conditions under which it is possible to extend the infrared pulse tuning range or varying the soliton pulse characteristics such as the pulse duration.

2. Experimental set-up

The first step was to generate a supercontinuum by propagation of ultrashort pulses in a nonlinear fiber. In order to do this, pulses of 80 fs duration (FWHM) at 826 nm from a 94 MHz repetition rate mode-locked Ti:sapphire laser (a model NJA-4, CLARK-MXR Inc. Oscillator) were injected into a 2 m long PCF (NL-2.5-810, Blaze Photonics [23]) using a 40X microscope objective (Fig. 1). An isolator was used to avoid feedback into the laser. The PCF has a zero dispersion wavelength λ_{ZD} of 810 nm. As the input wavelength is slightly longer than the fiber λ_{ZD}, the pulses propagate in the anomalous dispersion regime, and therefore soliton formation is possible [24]. An 8 mm focal length aspheric lens was placed at the PCF output for out-coupling the supercontinuum in a collimated beam.

A spectral filtering system that does not introduce extra dispersion was implemented in order to filter the longest wavelength soliton. This consists of an 1200 grooves/mm diffraction grating, and a 200 mm focal length lens, together with a variable slit and a mirror, as shown in Fig. 2. The variable slit and the mirror were mounted on a x-y translation stage. The supercontinuum frequencies were separated by the diffraction grating and sent to the frequency selector (variable slit) through the lens. The selected pulse is reflected

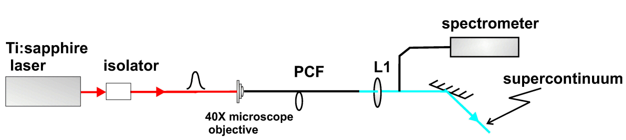

FIGURE 1. Experimental setup for supercontinuum generation.

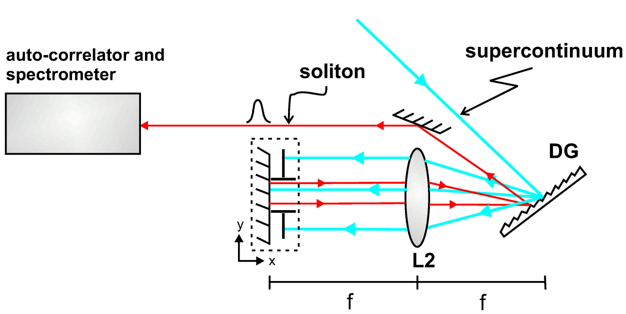

FIGURE 2. Experimental setup for soliton filtering system.

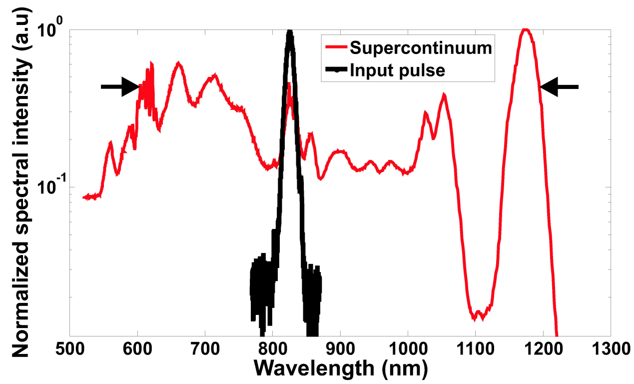

FIGURE 3. Supercontinuum and input pulse spectrum for 152 mW PCF output power.

by the mirror and sent back to the lens and grating. This is a folded version of the usual $4f$ system employed to manipulate the spectral phase of pulses [25, 26]. Given that the grating-lens, and lens mirror distances are equal to the focal length of the lens f, no chirp is introduced, and the pulse frequencies are transversely distributed in the y direction in the mirror plane.

After exiting this set-up, the selected soliton is directed either to an spectrum analyzer (HP 70951A), or a two-photon absorption based autocorrelator [27], in order to measure its spectrum and duration respectively.

The input Ti:sapphire laser pulses have an spectral width $\Delta\lambda$ (FWHM) of 14 nm, corresponding to a $\Delta\nu = 6.16$ THz, and their measured duration (FWHM) was $\tau_p = 80$ fs, giving a $\Delta\nu\tau_p$ product of 0.49. If we assume that pulses have a sech^2 temporal profile, the time-frequency product must satisfy the condition $\Delta\nu_p\tau \geq 0.315$ [28]. This indicates that input pulses are slightly chirped, which is important because it has been demonstrated that chirp in the input pulses can affect significatively the span of the generated continuum and hence the central wavelength of the generated solitons [11].

3. Results

3.1. Supercontinuum generation

Figure 3 shows the supercontinuum spectrum obtained for an average power measured at the PCF output of 152 mW, corresponding to a pulse energy of 1.61 nJ and 24.3 kW peak power. Note that the generated supercontinuum has a spectral width of about 590 nm; the input pulse spectrum is also shown in this figure. As it is expected in the anomalous dispersion regime, the fiber output presents a complex spectral structure in which it is possible to identify the infrared solitonic and visible dispersive wave components [7]. A well-defined spectral feature around 1180 nm is clearly appreciated in Fig. 3, which corresponds to the longest wavelength self-frequency shifted soliton.

The soliton shift towards longer wavelengths, is a function of the optical average power coupled into the PCF. Neutral density filters were used for adjusting the input average

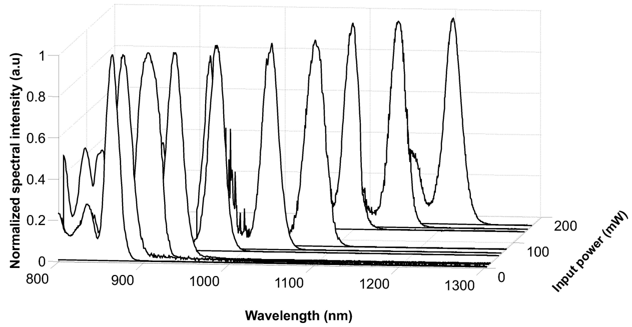

FIGURE 4. Experimental recorded supercontinuum spectra for several input average powers.

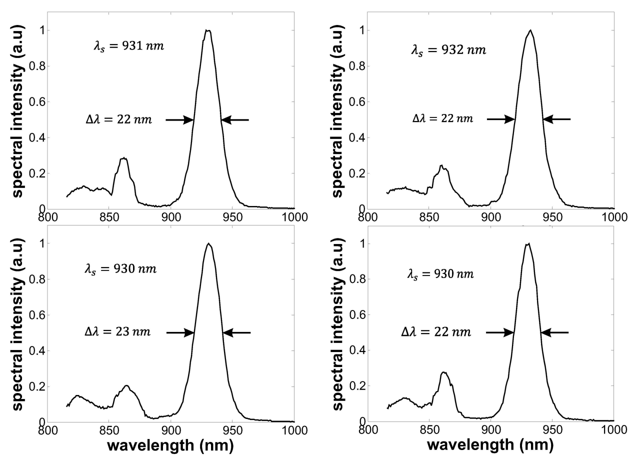

FIGURE 5. Stability test of the continuum. The experimental spectra were obtained for an input average power of 19 mW recorded with a 5 minute period between each one.

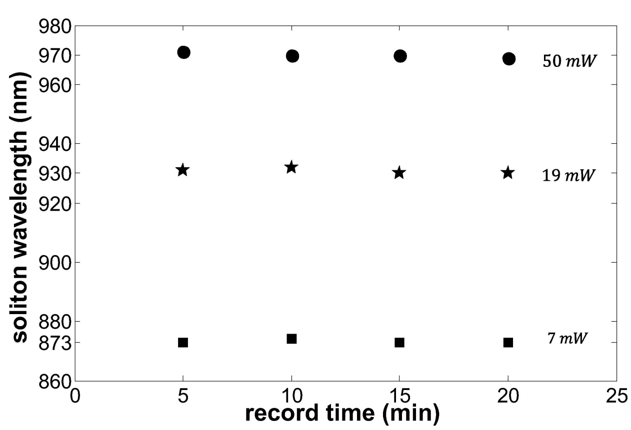

FIGURE 6. Stability test of the continuum. Soliton central wavelength as a function of time for three different input power (7, 19, and 50 mW).

power launched into the fiber. Fig. 4 shows the infrared part of the experimental supercontinuum spectra for different input average powers. We are interested in the longest wavelength features of the spectrum, so only the infrared portion is shown. The spectra show clearly that this portion of the continuum is comprised of well defined spectral peaks, corresponding to Raman solitons. In particular, note that the first fundamental soliton separated from the original pulse shifts roughly from 850 to 1200 nm for the considered input powers range. In order to test the stability of the continuum spectrum, several spectra were recorded for the same average power, with a 5 minute period between each one. Figure 5 shows the experimental spectra obtained for an input average power of 19 mW. Figure 6 shows the soliton central wavelength values as a function of time for three different input powers. The spectra was found to be very stable, with central wavelength (λ_s) remaining constant within $1-2$ nm over the whole period of time.

As it is well known, soliton formation results of the interplay between self-phase modulation, due to the instantaneous nonlinear response of the fiber, and group velocity dispersion effect. However, the soliton frequency shift to the infrared is produced by the Raman effect associated to a delayed nonlinear response, so that a proper theoretical description of soliton generation and its subsequent frequency shift, under our experimental conditions, requires numerical solution of the generalized nonlinear Schrödinger equation (GNSE) [29]

$$\frac{\partial A}{\partial z} + \frac{\alpha}{2}A - \sum_{j\geq 2}\frac{i^{j+1}}{j!}\beta_j\frac{\partial^j A}{\partial T^j} = i\gamma\left(1 + i\frac{1}{\omega_0}\frac{\partial}{\partial T}\right) \times \left[A(z,T)\int R(T')|A(z,T-T')|^2 dT'\right], \quad (1)$$

where $A(z,t)$ represents the time-domain electric field envelope, which has the form $A(0,t) = \text{sech}(t)\text{exp}(-iCt^2/2)$ at the fiber input, with C the chirp parameter. In Eq. (1) $R(t)$ is the nonlinear response function of fiber material which includes the electronic and Raman contributions (see Ref. 7). In order to numerically solve the Eq. (1), we first calculated the PCF dispersion by using the effective index model [30] and determined the nonlinear coefficient γ corresponding to the fundamental mode propagating inside the fiber. In our simulations we consider dispersion terms up to the sixth order and take into account the chirp of the input pulse.

Figures 7a and 7b show the experimental spectrum obtained for input average powers of 7 and 19 mW, respectively, while Figs. 7c and 7d correspond to spectra calculated by using Eq. (1) (only the infrared part of supercontinuum is shown). On the other hand, in Fig. 7e we present the input power dependence of the frequency shift of the longest wavelength fundamental soliton generated in the PCF. Note that we were able to simulate the supercontinuum generation up to a 55 mW input power, for which the input pulse becomes an 11th order soliton. It can be seen that the numerically obtained solutions exhibit a qualitative agreement with experimental results in the considered input power range. In particular, both the numerical and experimental data show evidence of:

i) the Raman-shift monotonically increases with the input power up to certain power value, above which it is possible to observe 'a saturation' of the SSFS [31], and

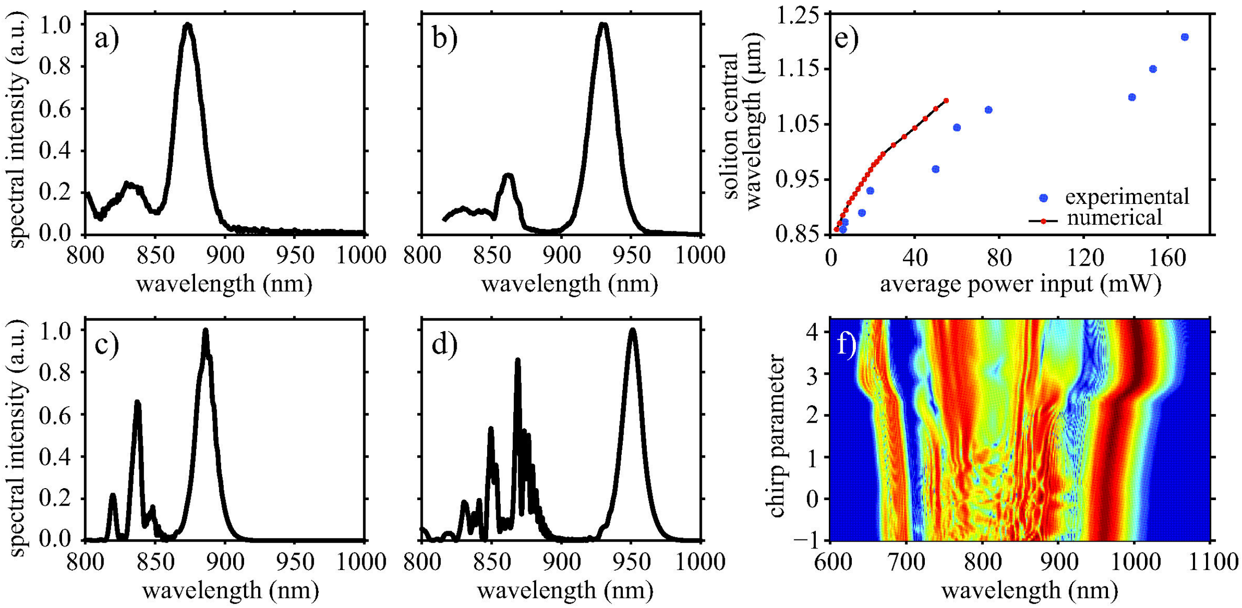

FIGURE 7. Experimental spectra obtained for a) $P_{av} = 7$ mW and b) $P_{av} = 19$ mW. c)-d) Numerical spectra relative to those in a) and b). e) Soliton frequency shift as a function of input average power. f) Supercontinuum generation as a function of input pulse chirp for a 25 mW pump power and 1 m fiber length.

ii) the spectral width of solitons (and hence the pulse duration) stays almost constant despite the input power variations.

This behavior is consistent with previously reported results [13]. The discrepancy between the experimental and theoretical results in relation with the frequency shift magnitude and bandwidth of generated solitons can be attributed to a lack of accurate knowledge of the input pulse chirp and fiber dispersion, in particular of the higher order dispersion coefficients.

In order to elucidate this point, we numerically analyze the frequency shift dependence with the input pulse chirp, under our experimental conditions. As it has been previously reported, there is an amount of positive chirp, which gives a maximum Raman-induced shifting, while holding all other parameters constant [11]. Figure 7f shows the dependence of the shift with input pulse chirp, for a 25 mW input power and a 1 m fiber length. If the input pulse is transform limited, the soliton, which experiences the greater SSFS, is centered at 962 nm. However, it can be seen that for $C = 3.5$ the soliton can be tuned around 1006 nm, which corresponds to an increase of 44 nm in the magnitude of the shift. A further increase in the C value leads to a decrease in the soliton central wavelength. Here, we assumed a fiber length $L = 1$ m (less than that used in the experiment) to illustrate that shorter fibers contribute to soliton generation with shorter pulse duration. In this case, the bandwidth of the solitons in which we are interested is about 20 nm.

3.2. Supercontinuum filtering

The generated continuum was then directed to the filtering system described in the experimental set-up section, in order to filter the soliton out of the spectrum. The width and position of the slit were adjusted to select the soliton. The selected spectral portion of the spectrum was then sent to the different instruments for pulse diagnostics, namely a spectrometer and an autocorrelator. Figure 8a shows the experimental filtered soliton obtained for a 15 mW input power, which is centered at $\lambda_s = 890$ nm and has a spectral width of $\Delta\lambda_s = 23$ nm. In this case, the average power associated to the filtered soliton was 6.5 mW, corresponding to a pulse energy of 0.07 nJ and a 1.41 kW peak power. The experimental auto-correlation trace showed in Fig. 8b gives a pulse length of 42 fs, leading to a time-bandwidth product of 0.37. Thus, the resulting pulse is very close to a transform limited one, as it is expected for a fundamental soliton. In the case reported on reference [13], the authors reported a constant average power of the soliton at 1 mW, which is below the power levels for the proposed applications in multiphoton microscopy, and considerably lower that what we report here. Added to this, they cannot get a soliton shift towards longer wavelengths, because they reach the limit of ’saturation’.

On the other hand, we used the theoretical spectra to model the soliton filtering process by applying a rectangular filter with a large enough bandwidth and then Fourier transforms to get the temporal profile and calculate the autocorrelation trace. For 15 mW input power, the calculated filtered soliton is shown in Fig. 8c while its corresponding calculated correlation trace appears in Fig. 8d. The calculated pulse duration was 60 fs, which is consistent with a transform limited pulse with a 16 nm bandwidth. Note that although the calculated soliton duration is larger than the measured one, the simulation predicts that our system can produce pulses much shorter than those launched into the fiber.

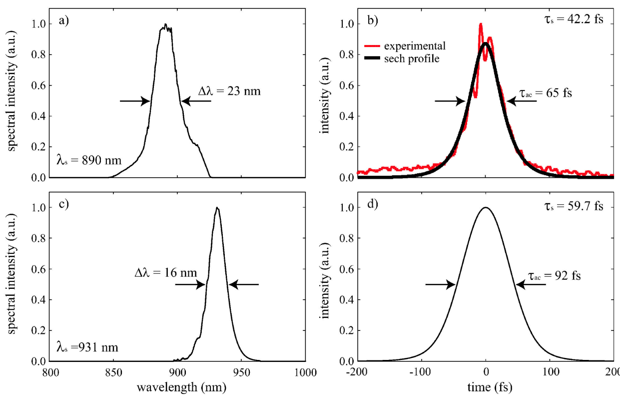

FIGURE 8. a) and b) Experimental spectral and temporal characteristics, respectively, for the filtered soliton for an average power coming out of the fiber of 15 mW. The soliton has an energy of 0.07 nJ and it is centered at 890 nm. c) and d) Theoretical spectrum and autocorrelation trace, respectively. The calculated pulse duration was 59.7 fs.

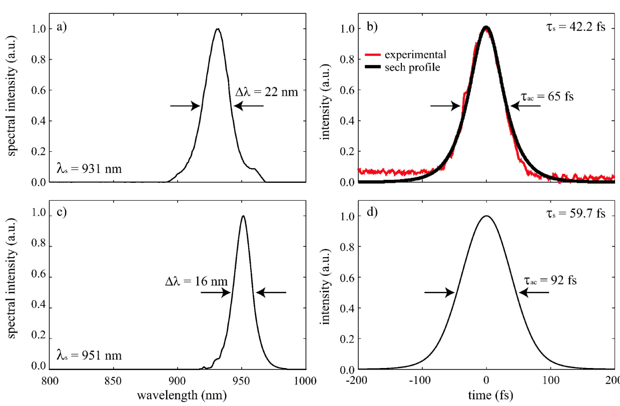

FIGURE 9. Experimental spectral and temporal characteristics for the filtered soliton for an average power of 19 mW. a) The soliton has a energy of 0.04 nJ and it is centered at 931 nm, b) Soliton duration (FWHM) was 42 fs. c) Theoretical soliton spectrum and d) calculated autocorrelation trace.

Tuning of the selected pulse is achieved by changing the input power and adjusting the filtering system. Figure 9a shows the filtered soliton spectrum for a fiber output power of 19 mW. The selected soliton pulse is now centered at 931 nm with a 3.6 mW average power, corresponding to a pulse energy of 40 pJ and 782 W peak power. The autocorrelation trace is shown in Fig. 9b, and the measured pulse duration was 42 fs. Considering the spectral width ($\Delta\lambda = 22$ nm) of Fig. 9a, the expected duration for a transform limited pulse is $\tau = 42$ fs, so that the filtered pulse is effectively a fundamental soliton. Figs. 9c and 9d show the theoretical spectral and temporal characteristics for the filtered soliton, respectively. In this case, the simulation yields a soliton duration of 60 fs, which is the same obtained in the case of Fig. 8. Note that the soliton average power is lower than in the previous case, this is because although the input power is increased, the energy is distributed over a wider spectral range.

Filtered pulses were obtained at different central wavelengths, the longest measured wavelength was 1100 nm, however, no auto-correlation traces were obtained for central wavelengths above 930 nm because the energy was not high enough for the autocorrelator. The pulse energies measured varied from 10 pJ at 993 nm to 3 pJ at 1100 nm, while the minimum measurable energy for the auto correlation was around 10 pJ, so the signal to noise ratio was very small for these wavelengths.

4. Conclusions

Tunable ultrashort laser pulses have been generated in the 850-1100 nm range by filtering the longest wavelength soliton component of the supercontinuum generated in a photonic crystal fibre. Tuning was achieved by varying the peak power of injected 80 fs pulses from a modelocked Ti:sapphire laser. Using the solitonic component of the supercontinuum allowed the extraction of very short nearly transformed limited pulses, with duration around 40 fs, and average powers ranging from 7 mW (or 70 pJ per pulse) at 890 nm, to 0.3 mW (3 pJ per pulse) at 1100 nm. The measured spectra and pulse durations are in very good agreement with theoretical calculations made including the effect of intra-pulse Raman scattering. It was numerically verified that we can extend the tuning range by optimizing the input pulse frequency chirp, and it is also possible to produce shorter soliton pulses by generating the super-continuum in a shorter fiber.

The wavelength range covered is very useful for applications such as second and third harmonic generation microscopy, where the generated signals need to be kept in the visible to avoid damage to living tissue or absorption in the microscope optics. It can also be useful as an excitation source tuned to maximize two-photon absorption excited fluorescence emission of certain dyes, for two-photon absorption fluorescence microscopy applications. Although the measured power levels can be considered low for certain applications, they are high enough for the multiphoton absorption microscopy techniques mentioned, where 1 mW on the sample plane is usually enough to get a good signal to noise ratio. The process can be made more efficient by replacing the grating in the folded $4f$ system used for filtering, by a prism, which has lower losses.

Acknowledgments

We want to acknowledge CONACYT-Mexico for partial funding for this work through Grant No. 46492

1. S.T. Sanders, *Appl. Phys. B-Lasers Opt.* **75** (2002) 799.
2. I. Hart *et al.*, *Opt. Lett.* **26** (2001) 608.
3. D.M. Brown, K. Shi, Z. Liu, and R. Philbrick, *Opt. Express.* **16** (2008) 8457.
4. J.K. Ranka, R.S. Windeler, and A.J. Stentz, *Opt. Lett.* **25** (2000) 25.
5. A.L. Gaeta, *Opt. Lett.* **27** (2002) 924.
6. J.M. Dudley, L. Provino, and N. Grossard, *J. Opt. Soc. Am. B.* **19** (2002) 765.
7. J.M. Dudley, G. Genty, and S. Coen, *Rev. Mod. Phys.* **78** (2006) 1135.
8. X. Liu *et al.*, *Opt. Lett.* **26** (2001) 358.
9. M.G. Banaee and J.F. *Young, J. Opt. Soc. Am. B* **23** (2006) 1484.
10. B.R. Washburn *et al.*, *Electron. Lett.* **37** (2001) 1510.
11. C.F. Cheng, X.F. Wang, and B.F. Shen, *Chin. Phys. Lett.* **21** (2004) 1965.
12. J.H. Lee, J.V. Howe, C. Xu, and X. Liu, *IEEE J. Sel. Top. Quantum Electron.* **14** (2008) 713.
13. M.E. Masip *et al.*, *Opt. Lett.* **34** (2009) 842.
14. R. Unruh *et al.*, *Opt. Express.* **14** (2006) 9825.
15. W.R. Zipfel, R.M. Williams, and W.W. Webb, *Nat. Biotechnol.* **21** (2003) 1369.
16. P.J. Campagnola, M. Wei, A. Lewis, and L.M. Loew, *Biophys. J.* **77** (1999) 3341.
17. A. Zoumi, X. Lu, G.S. Kassab, and B.J. Tromberg, *Biophys. J.* **87** (2004) 2778.
18. D. Débarre and E. Beaurepaire, *Biophys. J.* **92** (2007) 603.
19. G. McConnell, *Opt. Express.* **12** (2004) 2844.
20. H.N. Paulsen, K.M. Hilligsøe, J. Thøgersen, S.R. Keiding, and J.J. Larsen, *Opt. Lett.* **28** (2003) 1123.
21. K. Isobe *et al.*, *Jpn. J. Appl. Phys. Part 2* **44** (2005) L167.
22. J.A. Palero, V.O. Boer, J.C. Vijverberg, H.C. Gerritsen, and H.J.C.M. Sterenborg, *Opt. Express* **13** (2005) 5363.
23. Crystal Fibre, “NL-25-810 data sheet”, http://www.nktphotonics.com/files/files/NL-25-810.pdf
24. A.V. Husakou and J. Herrmann, *Phys. Rev. Lett.* **87** (2001) 203902.
25. D. Yelin, D. Meshulach, and Y. Silberberg, *Opt. Lett.* **22** (1997) 1793.
26. J.L.A. Chilla and O.E. Martinez, *Opt. Lett.* **16** (1991) 39.
27. M. A. García-Arthur, R. Rangel-Rojo, N. Jamasbi, and M. Mohebi, *Rev. Mex. Fís.* **49** (2003) 258.
28. J.C. Diels and W. Rudolph, *Ultrashort laser pulse phenomena* (Academic Press, San Diego, CA, 1996).
29. G.P. Agrawal, *Nonlinear Fiber Optics* (Academic Press, San Diego, CA, 1996).
30. K. Garay-Palmett *et al.*, *Optics Express* **15** (2007) 14870.
31. N. Nishizawa, Y. Ito and T. Goto, *IEEE Photon. Technol. Lett.* **14** (2002) 986.